

# An inexpensive widely available material for 4%wt reversible hydrogen storage near room temperature

Tod A. Pascal<sup>1,2</sup>, Christopher Boxe<sup>3</sup> and William A Goddard III<sup>1,2</sup>

<sup>1</sup>Material and Process Simulation Center, California Institute of Technology, Pasadena, CA USA

<sup>2</sup>Graduate School of EEWS (WCU), Korea Advanced Institute of Science and Technology, Daejeon, Korea

<sup>3</sup>Earth and Planetary Science Division, NASA Jet Propulsion Labs, Pasadena, CA USA

## Supporting Information

### I. Methods and Procedures

#### Force field fitting

Classical two and three body potentials were used to describe the various interactions in our system. The H<sub>2</sub> – H<sub>2</sub> and H<sub>2</sub> – H<sub>2</sub>O interactions were described using electrostatic interactions assuming fixed charges:

$$E_{coul} = \frac{q_i q_j}{\epsilon r_{ij}} \quad (1)$$

Where  $1/\epsilon = 14.399$  when  $E$  is in kcal,  $r_{ij}$  is in Å and the charge is in electron units. We use the Exponential-6 potential (Exp6 or Buckingham potential) to describe the weak van der Waals (vdW) forces:

$$E_{vdw} = Ae^{-CR} - b/R^6 = \frac{D_v}{(\xi - 6)} \{6e^{\xi(1-\rho)} - \xi\rho^{-6}\}, \quad \rho = \frac{r_e}{r_{ij}} \quad (2)$$

The anisotropy of the H<sub>2</sub> – H<sub>2</sub>O interactions was captured using the Dreiding-like<sup>1</sup> “Hydrogen – bond” between the H<sub>2</sub> bond-midpoint (the “donor”), the H atom on H<sub>2</sub> and the oxygen on H<sub>2</sub>O:

$$E_{hbond} = D_e \{5\rho^{-12} - 6\rho^{-10}\} \cos^p(\theta) \quad (3)$$

We first optimized the H<sub>2</sub> – H<sub>2</sub>O parameters by fitting the *ab-initio* potential energy surface of Phillips et al<sup>2</sup> which was calculated at the CCSD(T) level and the augmented, quadruple zeta aug-cc-pVQZ basis set of Dunning<sup>3</sup>, expected to yield accurate vdw parameters. The H<sub>2</sub>O – H<sub>2</sub>O interactions were described using the TIP4P-ice rigid water model<sup>4</sup>, validated to reproduce the melting temperature of ice Ih at STP, and not reoptimized here. The parameters were optimized using a Newton-Raphson minimization scheme. Thus writing  $\zeta$  as the set of observables we require the forcefield to reproduce, i.e.

$$\{\zeta\} = \left\{ r, \Theta, \Phi, \theta', \phi', E, \frac{\partial E_i}{\partial R_i} \right\} \quad (4)$$

is a function of the  $\text{H}_2 - \text{H}_2\text{O}$  equilibrium distance ( $r$ ),  $\text{H}_2$  relative orientation to  $\text{H}_2\text{O}$  ( $\Theta$ ,  $\Phi$ ),  $\text{H}_2$  absolute orientation ( $\theta'$ ,  $\phi'$ ) (see figure S1), total binding energy ( $E$ ) and the atomic forces  $\left(\frac{\partial E_i}{\partial R_i}\right)$  for atom  $i$  (by requiring zero total force be at the various minima). We then minimize the residual function  $R$ :

$$R(\{\zeta\}) = \sum_{i=1}^N w_i \left[ R_i^{\text{calc}}(\{\zeta\}) - R_i^{\text{obs}}(\{\zeta\}) \right]^2 \quad (5)$$

where  $N=84$  is the number of configurations used in the fit and  $w_i$  is the weighting factor. Typical values for weighting factor are 10 for the distances and orientations, 100 for the energies and 250 for the forces. This optimization lead to the parameters listed in Table 1, including a charge of +0.36535 on the H atoms of  $\text{H}_2$  (-0.7307 e- on the bond midpoint). These  $\text{H}_2$  charges are lower than the +0.47e- required to reproduce the experimental quadrupole moment<sup>5</sup> of -0.237 a.u., a natural consequence of our choice of fixed point-charges and the TIP4/ice water model.

We then optimized the  $\text{H}_2 - \text{H}_2$  vdW parameters by fitting to the *ab-initio* energy surface of Patkowski et. al.<sup>6</sup> which was calculated at the CCSD(T)/aug-cc-pV5Z+ (augmented quintuple zeta basis set) level expected to yield accurate vdw parameters.

### **Grand Canonical Monte-Carlo Simulations**

To predict the loading (pressure versus temperature) we used the grand canonical Monte Carlo (GCMC) method as implemented in the Sorption module of the Cerius2<sup>7</sup>. Our new FF in Table 1 was used to describe van der Waals interactions of  $\text{H}_2$  in the  $\text{H}_2\text{O}$  systems. In order to obtain an accurate measure of  $\text{H}_2$  loading, we used 10,000,000 Monte Carlo configurations to compute the average loading for each p and T, with an equal Translational/Rotational move probability and Creation/Destruction probability ratio of 2:1. The sorbent model is a three-dimensional, hexagonal ice structure ( $5 \times 5 \times 5$  supercell) consisting of 1500  $\text{H}_2\text{O}$  molecules ( $a=b=39.1\text{\AA}$ ,  $c=36.8\text{\AA}$ ,  $\alpha=\beta=90^\circ$ ,  $\gamma=120^\circ$ ). In all simulations, periodic boundary conditions are applied.

### **Molecular Dynamics Simulations**

All simulations were performed using the LAMMPS<sup>8,9</sup> simulation engine, which affords the flexibility of using various forcefields in a common framework. We had previously modified LAMMPS to include the full Dreiding FF, including 3-body HB<sup>10</sup>. Long-range coulombic interactions were calculated using the particle-particle particle-mesh Ewald method<sup>11</sup> (with a precision of  $10^{-5}$  kcal/mol), while the vdW interaction were computed with a cubic spline (inner cutoff of  $11\text{\AA}$  and an outer cutoff of  $12\text{\AA}$ ). We used the spline to guarantee that the energies and forces go smoothly to zero at the outer cutoff, preventing energy drifts that might arise from inconsistent forces. We also tested the effect of the vdW cutoff by computing the energy of a bulk  $\text{H}_2 - \text{H}_2\text{O}$  system (100 bar and 100K) with cutoffs ranging from 8 to  $20\text{\AA}$  and found converged results at  $12\text{\AA}$ .

The  $\text{H}_2$  molecules were treated as rigid bodies according to the schemes of Miller et. al.<sup>12</sup> and Kamberaj et. al.<sup>13</sup>. The O-H bonds and H-O-H angles on the TIP4P-ice waters were constrained

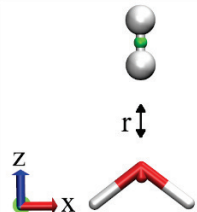
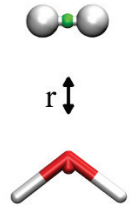
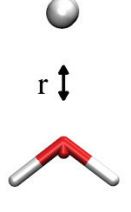
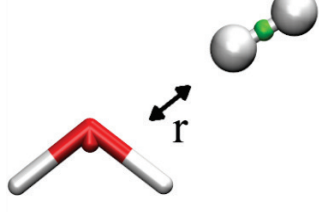
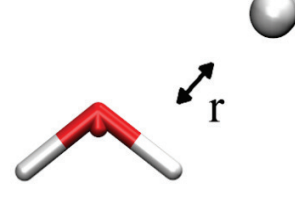
according to the SHAKE algorithm (convergence tolerance  $1.0\text{E-}5$  achieved over a maximum of 50 iterations).

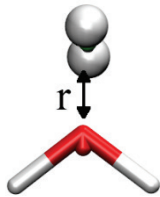
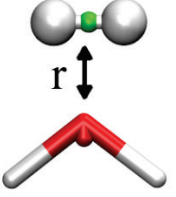
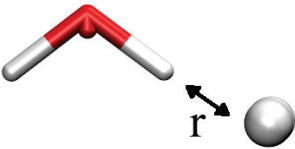
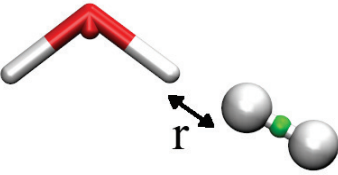
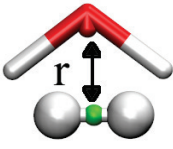
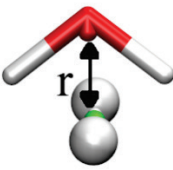
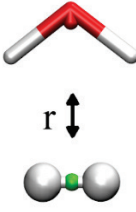
The starting structure for each MD simulation was obtained from our GCMC calculations. Slab geometries were generated by centering the optimized GCMC  $\text{H}_2/\text{H}_2\text{O}$  structures in a  $200\text{\AA}$  high box, with  $\text{H}_2$  molecules placed in the free space to match the required pressure. To rapidly equilibrate these systems, we used our standard procedure<sup>14-16</sup>: after an initial conjugant gradient minimization to an RMS force of  $10^{-4}\text{kcal/mol/\AA}$ , the system was slowly heated from 0K to the desired temperature over a period of 100 ps using a Nose-Hoover thermostat in the constant temperature, constant volume canonical (NVT) ensemble. The temperature coupling constant was 0.1 ps and the simulation timestep was 1.0 fs.

This equilibration was followed by 1ns of constant-pressure, constant-temperature (NPT) dynamics at the desired temperature and pressure. The system was adjusted in the x and y directions independently (the z direction was not adjusted) based on the stresses on the water molecule only. This procedure seems adequate to maintain the initial pressure of the slab geometry while simultaneously allowing the water molecules to adjust to the presence of the  $\text{H}_2$  molecules. The temperature coupling constant was 0.1 ps while the pressure piston constant was 2.0 ps. The equations of motion used are those of Shinoda et al.<sup>17</sup>, which combine the hydrostatic equations of Martyna et al.<sup>18</sup> with the strain energy proposed by Parrinello and Rahman<sup>19</sup>. The time integration schemes closely follow the time-reversible measure-preserving Verlet integrators derived by Tuckerman et al.<sup>20</sup>. Production dynamics was then run for a further 50ns in the micro-canonical (NVE) ensemble, with coordinates and velocities saved every 10ps for post-trajectory analysis.

## II. Tables

Table S1: Comparison of *ab-initio* and force field  $\text{H}_2 - \text{H}_2\text{O}$  interaction energies. The *ab-initio* data represent a rigid scan of the 5-D potential energy surface (14 unique configurations), with the center of mass distances sampled at 6 unique points.

	$\Theta$	$\Phi$	$\theta'$	$\phi'$	$R (\text{\AA})$	Interaction energies (kcal/mol)		
						FF	QM	Diff
	0	0	0	0	2.11662	19.1829	8.3819	-10.801
					2.64577	1.4659	0.19888	-1.26702
					3.17493	-0.5292	-0.56738	-0.03818
					3.70409	-0.4527	-0.39051	0.06219
					4.23324	-0.2688	-0.2259	0.0429
					6.34986	-0.0416	-0.03617	0.00543
	0	0	90	0	2.11662	9.5934	9.58899	-0.00441
					2.64577	0.993	1.36821	0.37521
					3.17493	-0.0279	0.15397	0.18187
					3.70409	-0.0623	0.02156	0.08386
					4.23324	-0.0242	0.0165	0.0407
					6.34986	0.0066	0.00995	0.00335
	0	0	90	90	2.11662	9.3769	8.66056	-0.71634
					2.64577	0.9013	1.13801	0.23671
					3.17493	-0.0721	0.06553	0.13763
					3.70409	-0.0856	-0.02059	0.06501
					4.23324	-0.0374	-0.0058	0.0316
					6.34986	0.0044	0.00669	0.00229
	60	0	60	0	2.11662	19.5013	8.91128	-10.59
					2.64577	1.8217	0.5791	-1.2426
					3.17493	-0.2727	-0.27274	-0.00004
					3.70409	-0.2926	-0.1998	0.0928
					4.23324	-0.1701	-0.10731	0.06279
					6.34986	-0.0217	-0.01398	0.00772
	60	0	90	90	2.11662	8.3524	6.19234	-2.16006
					2.64577	0.5424	0.3407	-0.2017
					3.17493	-0.2255	-0.2002	0.0253
					3.70409	-0.1658	-0.12992	0.03588
					4.23324	-0.0848	-0.06187	0.02293
					6.34986	-0.0053	-0.00306	0.00224

	60	90	60	90	2.11662	9.9075	7.95963	-1.94787
					2.64577	0.6375	0.28783	-0.34967
					3.17493	-0.3075	-0.52352	-0.21602
					3.70409	-0.2368	-0.36949	-0.13269
					4.23324	-0.1329	-0.20978	-0.07688
					6.34986	-0.0169	-0.02945	-0.01255
	60	90	90	0	2.11662	8.502	10.09147	1.58947
					2.64577	0.8179	1.62662	0.80872
					3.17493	-0.0657	0.22104	0.28674
					3.70409	-0.0802	0.03019	0.11039
					4.23324	-0.0372	0.01207	0.04927
					6.34986	0.0021	0.0066	0.0045
	120	0	90	90	2.11662	19.4105	14.93764	-4.47286
					2.64577	0.9458	0.86811	-0.07769
					3.17493	-0.5136	-0.54353	-0.02993
					3.70409	-0.3549	-0.37916	-0.02426
					4.23324	-0.1918	-0.19868	-0.00688
					6.34986	-0.0235	-0.02182	0.00168
	120	0	120	0	2.11662	78.3029	37.56735	-40.7356
					2.64577	9.665	5.33627	-4.32873
					3.17493	1.2593	0.78813	-0.47117
					3.70409	0.2386	0.16283	-0.07577
					4.23324	0.0891	0.07665	-0.01245
					6.34986	0.0179	0.01996	0.00206
	120	90	90	0	2.11662	7.3932	9.65081	2.25761
					2.64577	0.5027	1.45104	0.94834
					3.17493	-0.194	0.10467	0.29868
					3.70409	-0.1548	-0.05172	0.10308
					4.23324	-0.0872	-0.04152	0.04568
					6.34986	-0.0111	-0.00586	0.00524
	120	90	120	90	2.11662	9.5039	9.56855	0.06465
					2.64577	0.9323	1.00437	0.07207
					3.17493	-0.0526	-0.16555	-0.11295
					3.70409	-0.0776	-0.17167	-0.09407
					4.23324	-0.036	-0.09024	-0.05424
					6.34986	0.0025	-0.00294	-0.00544
	180	0	90	0	2.11662	9.4415	11.69064	2.24914
					2.64577	0.53	1.35937	0.82937
					3.17493	-0.293	-0.10751	0.18549
					3.70409	-0.2253	-0.17898	0.04632
					4.23324	-0.1322	-0.11199	0.02021
					6.34986	-0.0206	-0.01678	0.00382

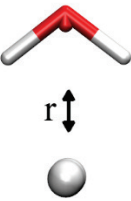
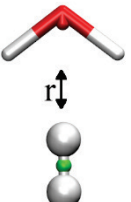
	180	0	90	90	2.11662	6.6713	9.04355	2.37225
					2.64577	-0.1011	0.67969	0.78078
					3.17493	-0.5079	-0.34242	0.16548
					3.70409	-0.3165	-0.27946	0.03704
					4.23324	-0.1762	-0.16123	0.01497
					6.34986	-0.0256	-0.0225	0.0031
	180	0	180	0	2.11662	21.0249	14.97472	-6.05018
					2.64577	2.6296	2.20692	-0.42268
					3.17493	0.2422	0.21009	-0.03211
					3.70409	0.0239	0.00781	-0.01609
					4.23324	0.0255	0.01801	-0.00749
					6.34986	0.0194	0.01858	-0.00082

Table S2: Shift in the melting temperature (K) for H<sub>2</sub> loaded ice Ih from our MD simulations and experiments<sup>21</sup>.

H <sub>2</sub> Pressure (bar)	Experimental			Simulation		
	Pure ice	H <sub>2</sub> loaded ice	$\Delta T_m$	Pure ice	H <sub>2</sub> loaded ice	$\Delta T_m$
1	273.15	273.15	0	272	271	0
200	271.40	271.6	+0.2	269	269	0
500	269.6	270.2	+0.6	265	266	+1
1000	264.5	265.8	+1.3	262	264	+2
1250	263.0	264.9	+1.9	257	260	+3
1500	260.5	264.2	+3.7	256	259	+3
1750	254.3	261.4	+7.1	250	255	+5
2000	250.9	260.1	+9.2	246	252	+8

### III. Figures

## H<sub>2</sub>O - H<sub>2</sub> coord. system

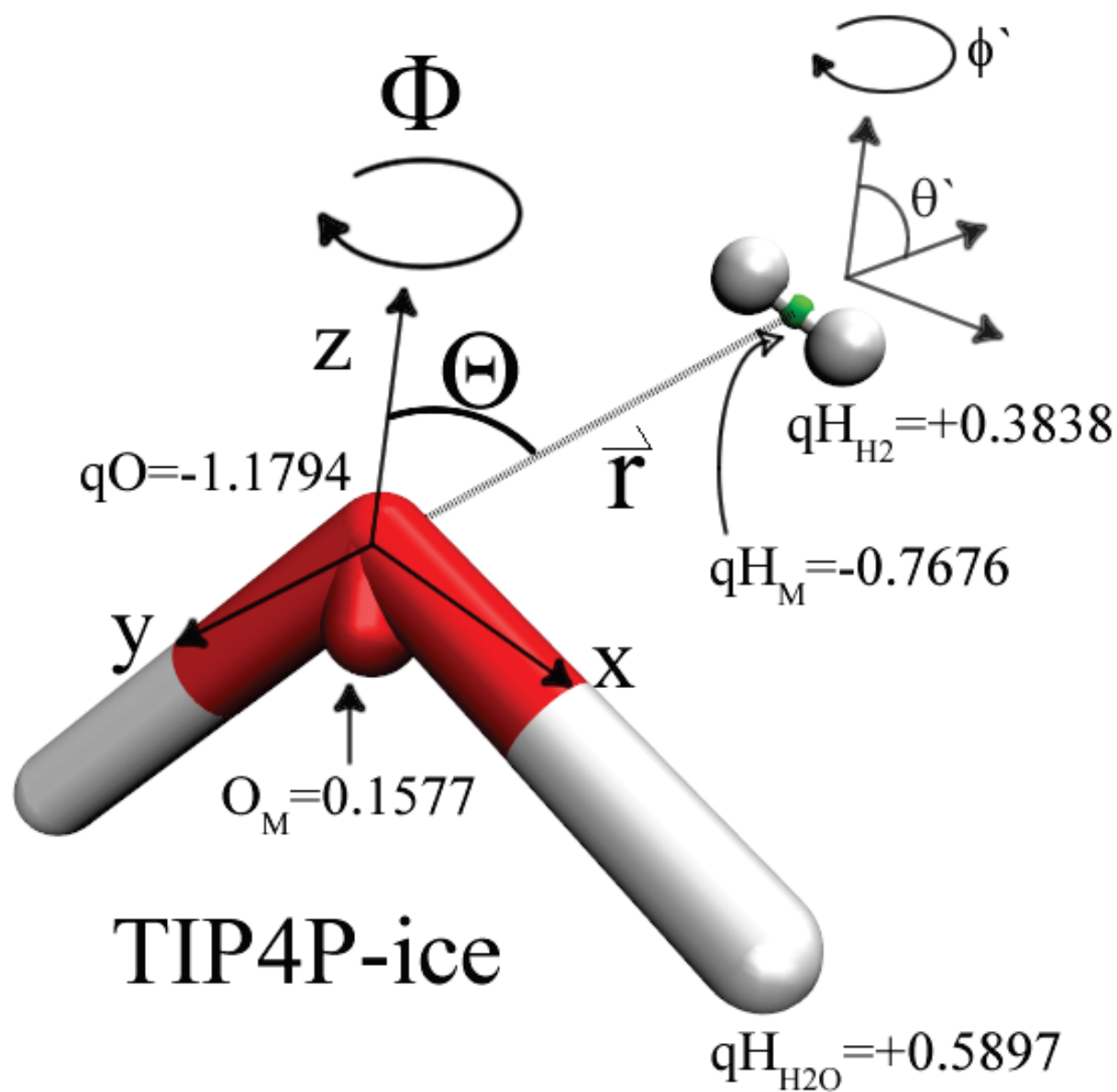


Figure S1: The H<sub>2</sub> – H<sub>2</sub>O coordinate systems used to fit the ab-initio potential energy surface of Phillips et al. (ref. 14 in the main text). The water-water interactions were described using the TIP4P-ice water model and not fitted. We optimized the H<sub>2</sub> charges and the H<sub>2</sub> – H<sub>2</sub>O van der Waals parameters, resulting in the parameters shown in Table 1.

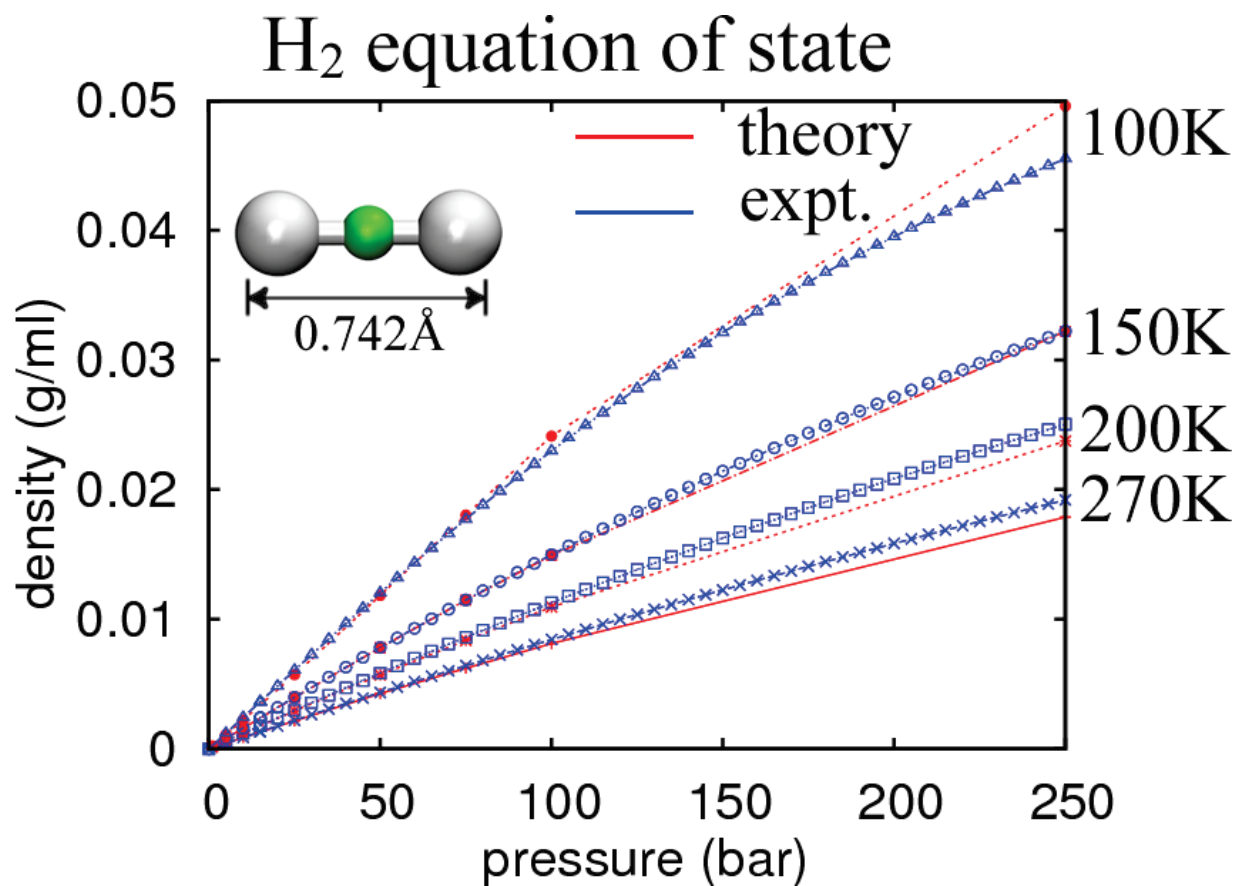


Figure S2: The H<sub>2</sub> equation of state for our three point H<sub>2</sub> model (red circles) compared to experiments (blue squares – ref. 16 in the main text). The charges on the atomic centers (+0.3828 e-) were determined by fitting the H<sub>2</sub> – H<sub>2</sub>O energy surface in figure S1. The H – H vdW parameters were re-optimized to reproduce the PES of the ab-initio energy surface of the H<sub>2</sub> dimer from Patkowski et. al. (ref 15 in the main text). The resulting parameters are listed in Table 1. The H<sub>2</sub> molecules in our simulations are taken to be rigid rotors, with an H – H bond length of 0.742 Å (7.42 pm).



## H<sub>2</sub> in ice Ih self diffusion constant

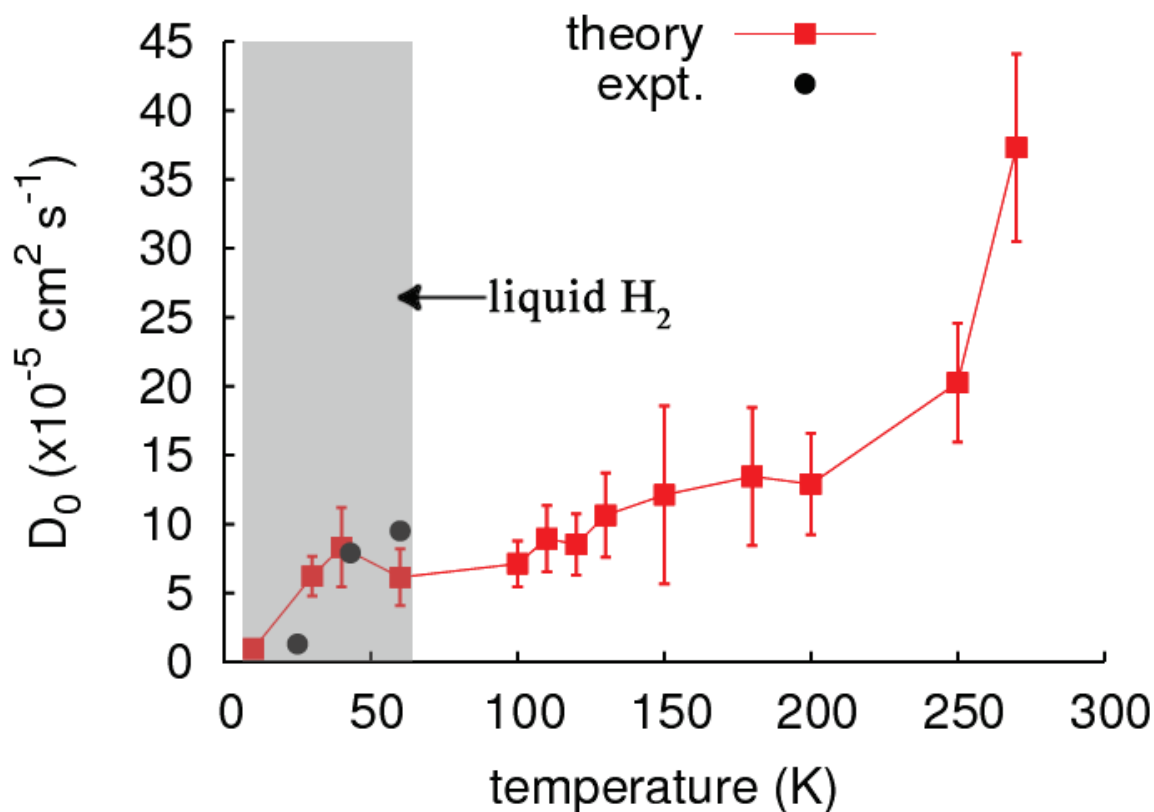


Figure S3: The self-diffusion constant of H<sub>2</sub> in ice Ih from our MD simulations (red squared line) compared to the low temperature experiments of Strauss et. al (ref 5 - black dots). The experimental data assumes that H<sub>2</sub> is a liquid from 0 – 77K. Our simulation results are obtained from 3D periodic calculations of the H<sub>2</sub> mean squared displacement in 50 100ps windows over 5 ns MD at each temperature. At each temperature, we assumed an H<sub>2</sub> pressure of 128 bar in a cubic cell of 12,800 water molecules (initial cell dimensions of 7.1 x 7.7 x 7.3 nm<sup>3</sup>) as determined from our GCMC calculations.

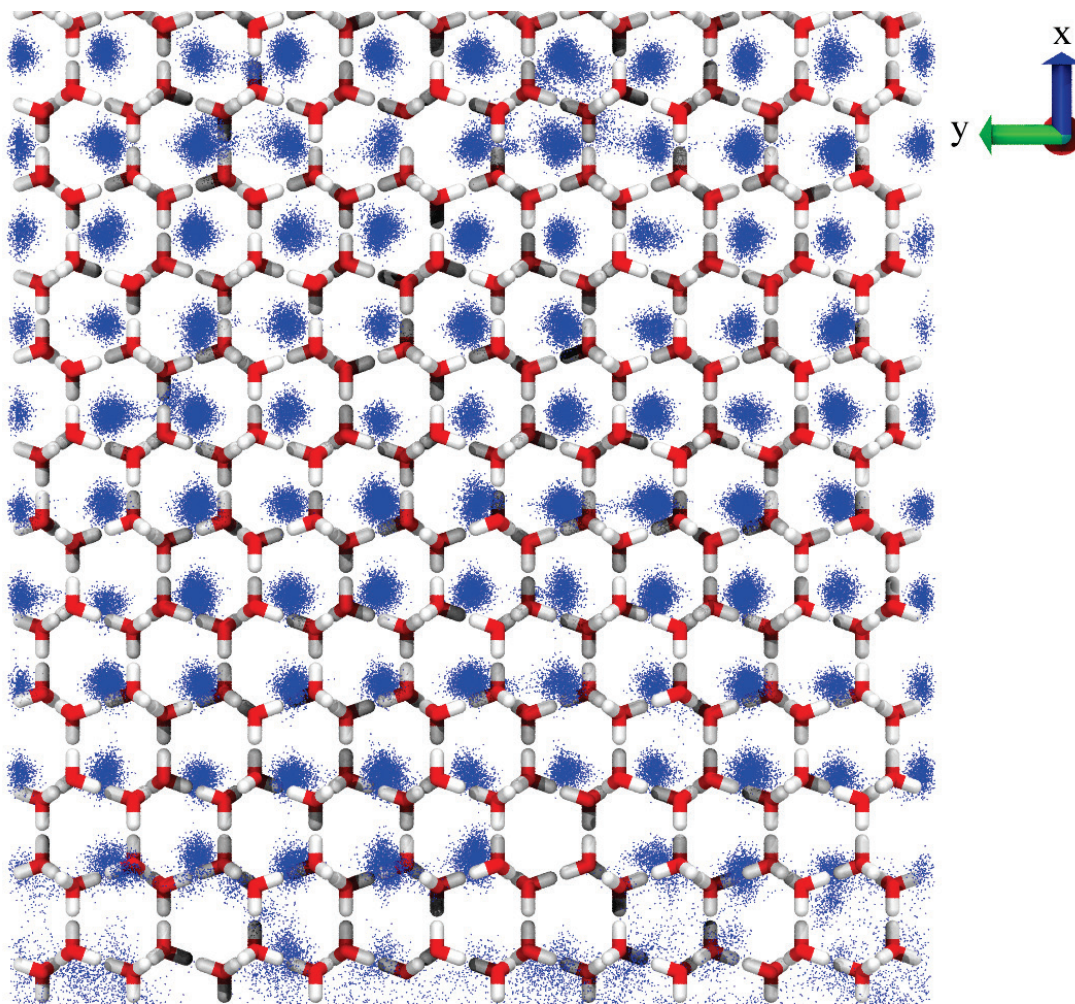


Figure S4: Two dimensional density profile of H<sub>2</sub> in ice Ih at 100K and 100bar projected along the x-axis

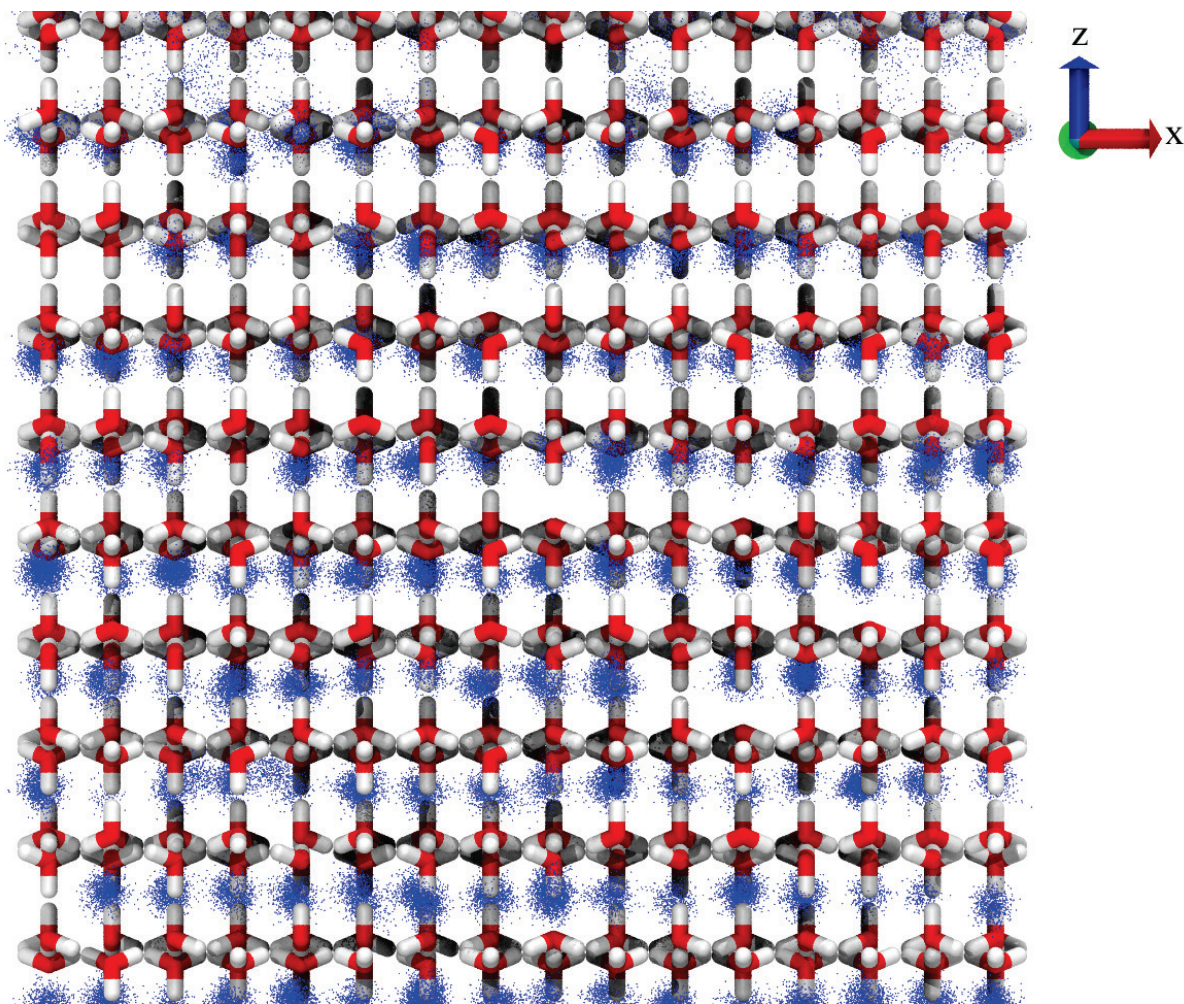


Figure S5: Two dimensional Density profile of H<sub>2</sub> stored in ice Ih at 100 bar and 100K projected along the y-axis.

## IV. References

- (1) Mayo, S. L.; Olafson, B. D.; Goddard, W. A. *J. Phys. Chem.* **1990**, *94*, 8897.
- (2) Phillips, T. R.; Maluendes, S.; Mclean, A. D.; Green, S. *J. Chem. Phys.* **1994**, *101*, 5824.
- (3) Dunning, T. H. *J. Chem. Phys.* **1989**, *90*, 1007.
- (4) Abascal, J.; Sanz, E.; Fernandez, R.; Vega, C. *The Journal of Chemical Physics* **2005**, *122*, 234511.
- (5) Flygare, W. H.; Benson, R. C. *Molecular Physics* **1971**, *20*, 225.
- (6) Patkowski, K.; Cencek, W.; Jankowski, P.; Szalewicz, K.; Mehl, J. B.; Garberoglio, G.; Harvey, A. H. *J. Chem. Phys.* **2008**, *129*.
- (7) Cerius2 Molecular Modelling Software, Accelrys, San Diego
- (8) Plimpton, S. J.; Pollock, R.; Stevens, M. "Particle-Mesh Ewald and rRESPA for Parallel Molecular Dynamics Simulations"; Proc of the Eighth SIAM Conference on Parallel Processing for Scientific Computing, 1997, Minneapolis, MN
- (9) Plimpton, S. *J. Comput. Phys.* **1995**, *117*, 1.
- (10) Pascal, T. A.; Lin, S.-T.; Goddard Iii, W. A. *Physical Chemistry Chemical Physics* **2011**.
- (11) Hockney, R. W.; Eastwood, J. W. *Computer Simulation Using Particles*; Taylor & Francis: New York, 1989.
- (12) Miller Iii, T. F.; Eleftheriou, M.; Pattnaik, P.; Ndirango, A.; Newns, D.; Martyna, G. J. *The Journal of Chemical Physics* **2002**, *116*, 8649.
- (13) Kamberaj, H.; Low, R. J.; Neal, M. P. *The Journal of Chemical Physics* **2005**, *122*, 224114.
- (14) Maiti, P. K. P., Tod A.; Vaidehi, Nagarajan; Goddard, William A. *J. Nanosci. Nanotechnol.* **2007**, *7*, 1712.
- (15) Maiti, P. K.; Pascal, T. A.; Vaidehi, N.; Heo, J.; Goddard, W. A. *Biophys. J.* **2006**, *90*, 1463.
- (16) Maiti, P. K.; Pascal, T. A.; Vaidehi, N.; Goddard, W. A. *NUCLEIC ACIDS RES* **2004**, *32*, 6047.
- (17) Shinoda, W.; Shiga, M.; Mikami, M. *Physical Review B* **2004**, *69*.
- (18) Martyna, G. J.; Tobias, D. J.; Klein, M. L. *J. Chem. Phys.* **1994**, *101*, 4177.
- (19) Parrinello, M.; Rahman, A. *Journal of Applied Physics* **1981**, *52*, 7182.
- (20) Tuckerman, M. E.; Alejandre, J.; Lopez-Rendon, R.; Jochim, A. L.; Martyna, G. *J. J Phys a-Math Gen* **2006**, *39*, 5629.
- (21) Dyadin, Y. A.; Aladko, E. Y.; Udachin, K. A.; Tkacz, M. *Pol J Chem* **1994**, *68*, 343.